Article

Discovery Medicine 2023; 35(179): 1190–1201
https://doi.org/10.24976/Discov.Med.202335179.115

Autophagy-Related Gene *CXCR4* is a Potential Predictor of Prognosis and Immunotherapy Response for Gastric Cancer

Zhi Zhao[1,†], Qingli Fang[2,†], Longqin Wei[3], Jinquan Lin[1], Ruping Su[1], Ni Li[4,*]

[1]Department of Gastrointestinal and Hernia Surgery, People's Hospital of Guilin, 541002 Guilin, Guangxi, China
[2]Scientific Research Center, Guilin Medicine University, 541199 Guilin, Guangxi, China
[3]Department of Scientific Research, People's Hospital of Guilin, 541002 Guilin, Guangxi, China
[4]Health Management Center, People's Hospital of Guilin, 541002 Guilin, Guangxi, China
*Correspondence: xykz521@163.com (Ni Li)
[†]These authors contributed equally.
Published: 1 December 2023

Background: Autophagy is involved in the survival, differentiation, and activation of immune cell subsets. In this study, we determined the prognostic value and biological functions of autophagy genes in gastric cancer (GC).
Methods: The RNA sequencing dataset for gastric cancer was obtained. Differences in prognosis and enrichment pathways in non-negative matrix factorization (NMF) subclasses were analyzed. Next, we analyzed CXC chemokine receptor 4 (*CXCR4*) by differential expression, clinical value, immune effects, tumor mutation burden (TMB) values, somatic variants, and biological functions.
Results: NMF identified three subclasses. Among the three subclasses, there were differences in prognosis, immune cell infiltration, immune checkpoint genes, and enrichment pathways. Moreover, *CXCR4* level was elevated in most tumors, and high *CXCR4* level was related to poor prognosis in GC patients. *CXCR4* expression was significantly correlated with B cells, eosinophils, macrophages, and plasma cells. In *in vitro* experiment, *CXCR4* promoted GC cell proliferation.
Conclusions: Our results showed that *CXCR4* is a promising biomarker for predicting prognosis and response to immunotherapy in GC.

Keywords: *CXCR4*; autophagy; bioinformatics; immune infiltration; gastric cancer

Introduction

It is estimated that there are over 1 million new gastric cancer (GC) cases each year [1,2]. Due to the lack of effective biomarkers for early diagnosis, GC often progresses to advanced stages or even metastasis, and the median overall survival of these patients is less than 1 year [3].

Autophagy maintains genome integrity and removes aggregated proteins [4]. Autophagy can inhibit or promote tumor growth in different microenvironment [5]. Therefore, modulation of autophagy can be used as an effective treatment approach.

Tumor cells evade tumor immunity by suppressing the immune response [6–8]. Autophagy within tumor cells affects the survival, apoptosis, differentiation, and activation of immune cell subsets [9–11]. Thus, autonomous autophagy of tumor cells can alter tumor growth by regulating immune responses [12–14]. However, the specific role of autophagy in regulating the immune response in GC is not clear.

In this study, we determined the prognostic value of autophagy genes in GC and their biological functions. We used the non-negative matrix factorization (NMF) approach to characterize autophagy-related genes, and to explore their impact on the prognosis, immune microenvironment, and clinical features of GC [15–17].

Methods

Data Sources

The RNA sequencing data sets (raw counts) and clinical information of The Cancer Genome Atlas Stomach Adenocarcinoma (TCGA-STAD) were downloaded from the UCSC Xena website (https://xenabrowser.net/). Gene somatic mutation data (MAF files) of STAD cohorts were obtained from TCGA-STAD (https://www.cancer.gov/ccg/research/genome-sequencing/tcga). The Affymetrix microarray data sets GSE54129 were obtained from Gene Expression Omnibus (GEO) database (https://www.ncbi.nlm.nih.gov/geo/).

Identification of GC Subclasses

Human autophagy-related gene sets (http://autophagy.lu/index.html) were obtained for subsequent NMF clustering using the R package "NMF" (Version 1.19.0, Bioconductor, Boston, MA, USA). The value of k with the maximum cophenetic correlation coefficient was chosen as the optimal number of clusters.

Identification of Differential Expression Genes (DEGs)

Differentially expressed genes were screened via the limma package. The significant Differential Expression Genes (DEGs) were as follows: $|\log_2$ fold change (FC)$| \geq 1$ and adjusted p value < 0.05.

Tumor Mutational Burden (TMB)

Tumor mutational burden (TMB) is an emerging biomarker associated with response to immune checkpoint blocking (ICB) therapies. A higher TMB score has been associated with better immune therapy efficacy [18]. TMB scores were calculated for each sample using the "maftools" software package (Version 2.18, Bioconductor, Boston, MA, USA). Differences in TMB scores between the CXC chemokine receptor 4 (*CXCR4*) high- and low-expression groups were assessed using the Wilcoxon rank sum test.

Gene Set Variation Analysis (GSVA) and Enrichment Pathways Analysis

Gene Set Variation Analysis (GSVA) was used to estimate variation in gene set enrichment based on transcriptomic data. In our study, c2.cp.v7.5 gene sets were analyzed using the "GSVA" package (Version 1.50, Bioconductor, Boston, MA, USA). Differential analysis was conducted using the limma package, and the pathways with $|\log_2$ fold change (FC)$| > 0.5$ (adjusted $p < 0.05$) were defined as differential expression.

Estimation for Immune Score, Stromal Score, and ESTIMATE Score

The ESTIMATE package can calculate the immune score, stromal score, and estimate score of each GC sample to reflect the value of each corresponding component in the tumor microenvironment (TME). The higher the score, the more corresponding component.

Survival Analysis

Survival analysis was carried out using both R packages "survival" and "survminer" (Version 1.190, Bioconductor, Boston, MA, USA). Samples with survival time less than 1 month were removed from survival analyses.

Correlation Analysis of Subclasses with Clinicopathological Characteristics

To explore potential correlations with clinicopathological characteristics, we performed correlation analysis of each subclass with clinicopathological characteristics using the ggpubr R package (Version 2.10, Bioconductor, Boston, MA, USA).

Immune Cell Infiltration and Immune Checkpoint Gene Analysis

To assess the proportion of tumor immune infiltrating cells (TICs) in GC cases, CIBERSORT was used to estimate the proportion of 22 phenotypic immune cells in each GC specimen. The fraction of each immune cell enriched in NMF subtypes and *CXCR4*-expressing subtypes was compared. We obtained 47 immune checkpoint-related genes from a previous study [19]. Subsequently, we analyzed the differences between these genes in NMF subtypes and *CXCR4* expression subgroups using the Kruskal-Wallis rank sum test and the Wilcoxon rank sum test.

Cell Culture and Transfect with siRNA

Gastric cancer cell line HGC-27 was obtained from Chinese Academy of Sciences (Shanghai, China). The HGC-27 cell line was subjected to STR authentication and mycoplasma testing. HGC-27 was cultured in RPMI-1640 (B.N.: 8122741, Gibco, Carlsbad, CA, USA) with 10% FBS (B.N.: 22100706, EVERY GREEN, Hangzhou, China), 100 UI/mL penicillin, and 100 mg/mL streptomycin. Lipofectamine™ 2000 (B.N.: 2398587, Invitrogen, Carlsbad, CA, USA) was employed to transfect *CXCR4* small interfering RNA (siRNA) and control siRNA (B.N.: 33621327, RiboBio, Guangzhou, China) into GC cells. The target sequence for *CXCR4* siRNA was 5′-CCAUGAAGGAACCCUGUUUTT-3′. The target sequence for control siRNA was 5′-UUCUCGCCACGGUUCAACUTC-3′.

Transwell

CXCR4 siRNA and control siRNA were transfected in GC cells. After transfection for 24 h, the chamber was removed. After staining with crystal violet, non-invasive cells in the upper chamber were carefully removed with a cotton swab. The infiltrating cells were observed under an inverted microscope, and the number of cells in the different fields of view was counted.

Scratch Test

The GC cells were plated into 6-well plate at a density of 5×10^5 in each well. After the cells were adhered overnight, homogenous scratches were created mechanically with sterile pins in each well. After taking pictures of the scratches at 0 h underneath an inverted microscope, the 6-well plate was put back into the incubator. After 24 h, the scratches were photographed again. The scratch area was

calculated by Image J software (Version: 1.8.0.345, NIH, Bethesda, MA, USA).

MTT Assay

After transfection with *CXCR4* siRNA for 24 h, cell viability was evaluated by MTT (3-(4,5-Dimethylthiazol-2-yl)-2,5-diphenyltetrazolium bromide) assay according to the manufacturer's instruction. Each sample was tested in quadruplicate. The absorbance was measured at 450 nm with a microplate reader (Version: 800TS, Bio-Rad, Santa Clara, CA, USA).

Apoptosis Analysis

Apoptosis was determined using flow cytometry with the Annexin V-FITC Apoptosis Detection Kit, as described previously [20]. Briefly, cells were transfected *CXCR4* siRNA for 48 h. After harvesting, the cells were subject to flow cytometry analysis (B.N.: V657338000453, Becton, Dickinson and Company, San Jose, CA, USA).

Immunohistochemistry (IHC) Staining and Patient Samples

IHC staining was performed as described previously [21]. Primary antibodies against *CXCR4* (1:100, B.N.: AF6621, Beyotime, Shanghai, China) were used for IHC staining. The relative expression of *CXCR4* was determined by Image-Pro Plus version 7.0 (Media Cybernetics, Rockville, MD, USA). A total of 40 patients who were diagnosed with gastric carcinoma by the pathology department were enrolled in this study.

Statistical Analysis

The statistical analysis was carried out with SPSS Statistics version 22.0 (IBM SPSS Statistics, Chicago, IL, USA). The one-way ANOVA or Kruskal-Wallis test was used to test the significance of differences among the three groups. For comparison of two groups, the Mann-Whitney *U* or unpaired Student's *t*-test was used to test differences. Correlation tests were based on Pearson's or Spearman's correlation analysis. Kaplan–Meier was used for survival analysis, and log-rank tests were used for comparison of survival curves. Univariate Cox regression models were used to estimate hazard ratios (HRs) and 95% confidence intervals (CIs). Two-tailed p values < 0.05 were considered statistically significant.

Results

Difference in Autophagy-Related Genes between Normal and GC Tissues

In total, 222 autophagy-related genes were downloaded. Differences between normal and GC tissues in the autophagy-related genes landscape are shown in Fig. 1A. Based on the 32 normal samples and 375 tumor samples, a total of 28 differentially expressed, autophagy-related genes were identified compared to the normal group, 10 genes were markedly upregulated and 18 genes were downregulated (Fig. 1B). Principal component analysis (PCA) revealed the existence of significantly different expression patterns (**Supplementary Fig. 1**). In order to explore the effects of the 28 differentially expressed genes on GC, we conducted univariate Cox regression analysis. As a result, seven genes were found to promote the progression of GC, and one gene was found to inhibit the progression of GC (**Supplementary Table 1**).

NMF Identified Three Subclasses in GC

To identify GC subclasses based on autophagy-related genes, 222 autophagy-related genes were used as the basis of NMF analysis. The optimal k value was generated by calculating cophenetic correlation coefficients. Eventually, k = 3 was chosen as optimal number of clusters to achieve NMF analysis (Fig. 1C). The results showed that GC samples were divided into three subclasses. We performed Kaplan–Meier survival analyses. As a result, a significant prognostic difference was observed (Fig. 1D). To better characterize the difference among the three GC subclasses, differential analyses were conducted. As shown in Fig. 1E, the hierarchical clustering heatmap clearly showed differences in the profile of autophagy-related genes among the three subclasses. We further investigated the differences between GC subclasses and clinical characteristics. The differences between GC subclasses and clinical characteristics are shown in Fig. 1E.

Immune Infiltration and Immune Checkpoint Gene Analysis of GC Subclasses

Next, we used CIBERSORT to explore the immunologic landscape of GC subclasses. The immune composition of each GC sample was dissected into subsets based on 22 types of immune cells. In Fig. 2A, the proportion of each of the 22 types of immune cells in each sample is presented in the box plot. A significant difference was observed between subgroup 1 and the other two subgroups. Subgroup 1 had a higher level of memory B cells, naive B cells, activated dendritic cells, resting dendritic cells, macrophages M0, monocytes, plasma cells, resting memory CD4+ T cells, CD8+ T cells, gamma delta T cells, and regulatory T cells (Tregs) compared to subgroup 2 and subgroup 3 (Fig. 2A). In addition, we further explored the association between subclasses and 47 immune checkpoint genes from a previous study. The result showed that subgroup 1 exhibited higher expression levels for 31 immune checkpoint genes compared to subgroup 2 and subgroup 3 (Fig. 2B).

Enriched Pathways Analyses of Subclasses

To identify differences in enriched pathways among subclasses, we conducted GSVA analyses based on c2.cp.v7.5 gene sets. The result is shown in Fig. 2C. Al-

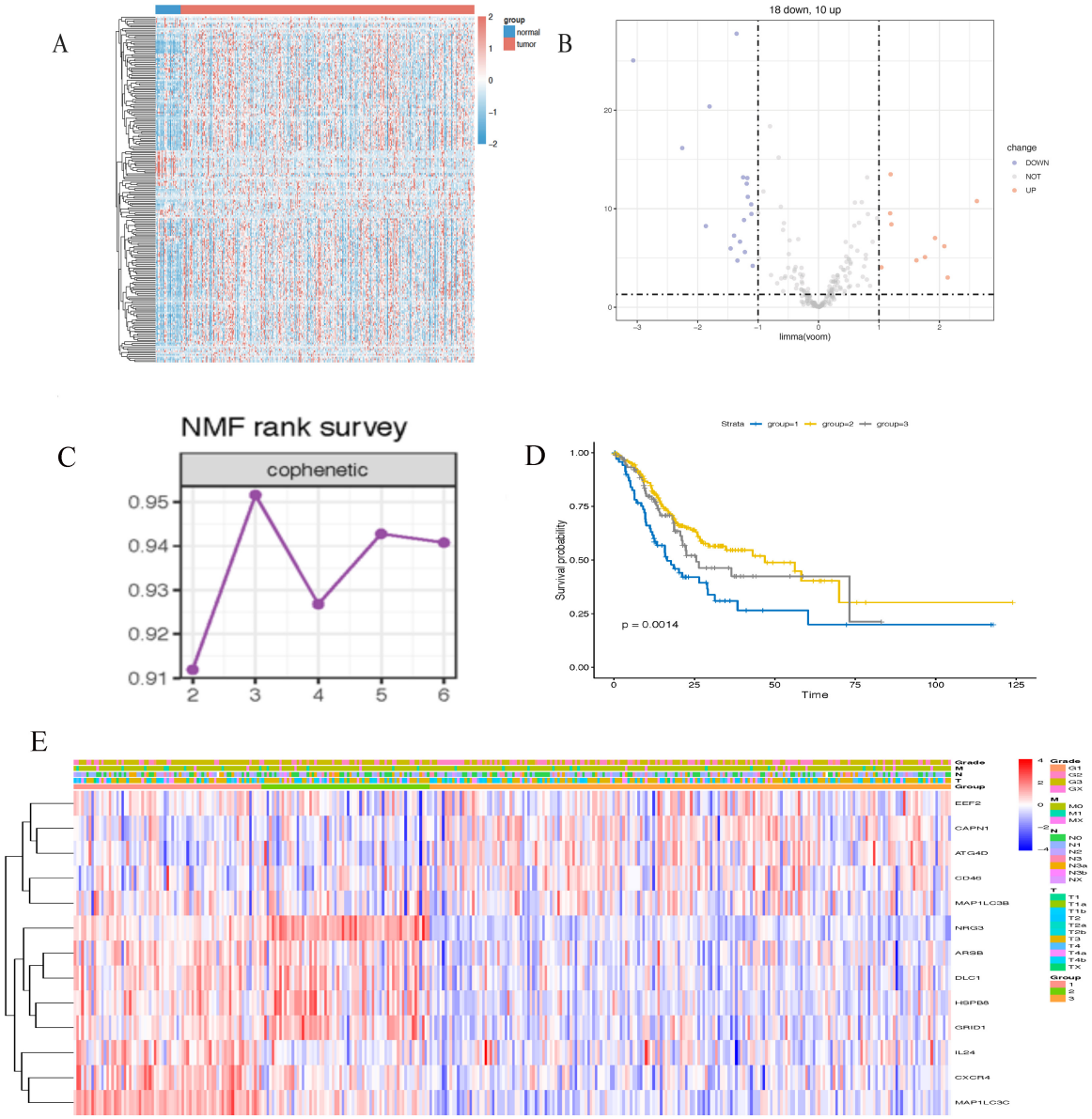

Fig. 1. The landscape of autophagy-related genes in GC samples and identification of subclasses in GC based on autophagy-related genes. (A) Hierarchical clustering of autophagy-related genes between normal and GC samples. (B) Volcano plot shows the differentially expressed 28 autophagy-related genes in GC. (C) The optimal number of clusters (k) was selected using the NMF clustering method. (D) Survival analysis was used to evaluate the different survival patterns between subclasses. (E) Heatmap of represented autophagy-related genes in the three subclasses. The correlation between their expression and clinical characteristics is shown. group 1, GC subclass 1; group 2, GC subclass 2; group 3, GC subclass 3. GC, gastric cancer; NMF, negative matrix factorization; *CXCR4*, CXC chemokine receptor 4; ATG4D, autophagy related 4D cysteine peptidase; DLC1, deleted in liver cancer 1.

though there were differences in many pathways between the three subclasses ($p < 0.05$), the $|\log_2 FC|$ of pathways was less than 0.5.

CXCR4 was Identified as a Hub Gene and was Correlated with Survival and Clinicopathological Characteristics in GC Patients

Eight genes with statistical significance were observed in 28 DEGs (**Supplementary Table 1**). However, among the 8 DEGs, only *CXCR4* was significantly upregulated ($p < 0.05$, $\log_2 FC > 1$, **Supplementary Table 2**). Moreover, among the 8 DEGs, ATG4D (autophagy related 4D cysteine peptidase), *CXCR4*, DLC1 (deleted in liver cancer 1), and GABARAPL2 (GABA(A) receptor-associated protein-like 2) were positively correlated with CD274 (**Supplementary Fig. 2**). *CXCR4* had the highest correlation with CD274. Besides, high *CXCR4* expression was significantly correlated with worse overall survival (OS; Fig. 3A). Meanwhile,

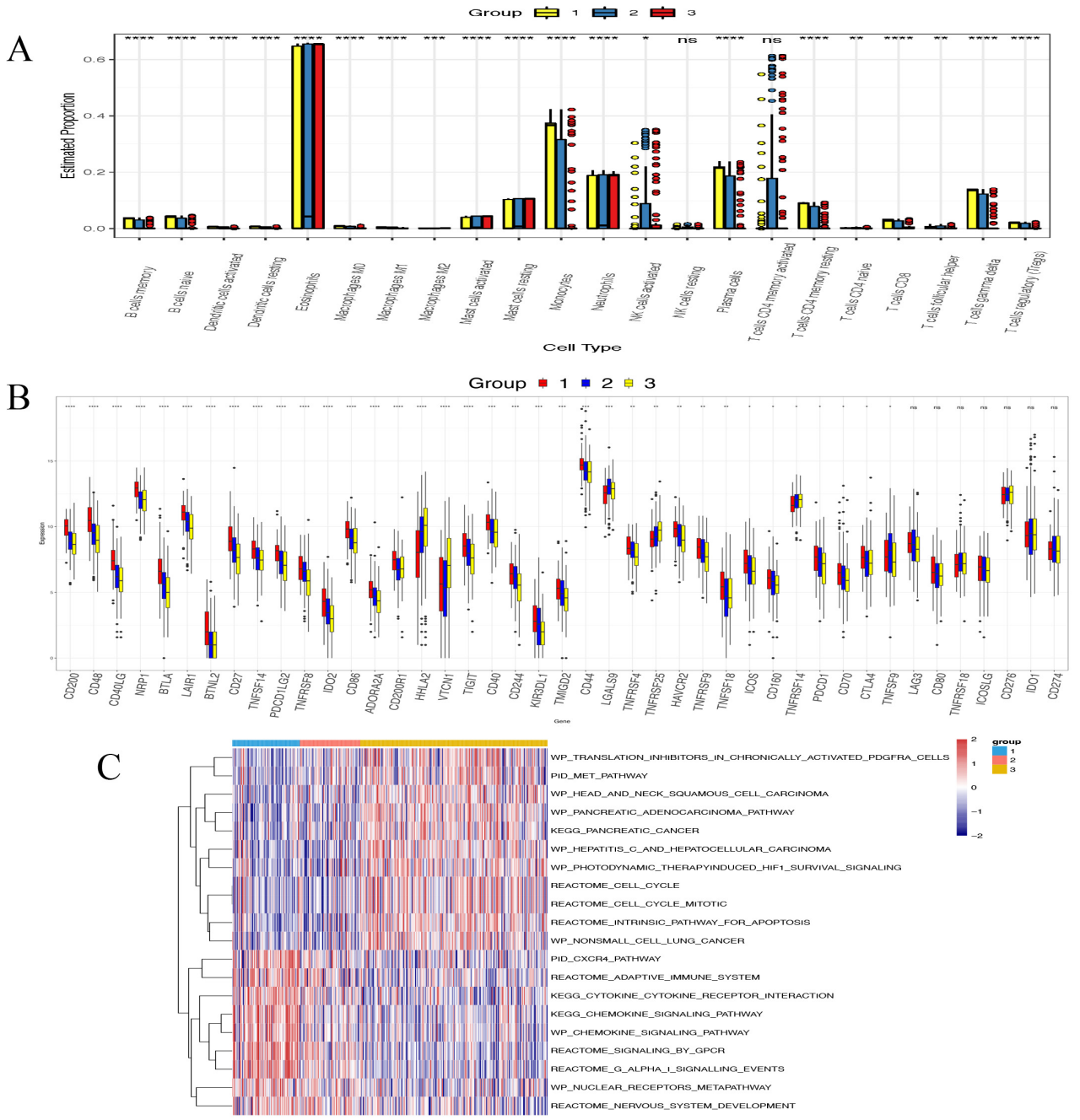

Fig. 2. Evaluation of tumor microenvironment (TME) immune cell infiltration characterization and enriched pathways analysis of GC subclasses. (A) Box plots for the association between GC subclasses and infiltration levels of immune cells. (B) The distribution difference of immune checkpoint genes among the GC subclasses. (C) The difference of enriched pathways in the GC subclasses. group 1, GC subclass 1; group 2, GC subclass 2; group 3, GC subclass 3. * $p < 0.05$; ** $p < 0.01$; *** $p < 0.001$; **** $p < 0.0001$; ns, not significant. CTLA4, cytotoxic T-lymphocyte-associated protein 4; PDCD1, programmed cell death protein 1; PDCD1LG2, recombinant programmed cell death protein 1 ligand 2.

CXCR4 was elevated in tumor samples (Fig. 3B). Next, we analyzed the *CXCR4* expression profile in 37 human cancers using the TIMER database. *CXCR4* expression was highly elevated in tumors (Fig. 3C). *CXCR4* expression was positively correlated with expression of CTLA4 (cytotoxic T-lymphocyte-associated protein 4), PDCD1 (programmed cell death protein 1) and PDCD1LG2 (recombinant programmed cell death protein 1 ligand 2) (Fig. 3D–G) in GC samples. Therefore, *CXCR4* was identified as a hub gene and selected for further study in GC patients. We further analyzed the correlation between *CXCR4* and clinicopathological characteristics. The *CXCR4* expression was significantly correlated with T stage and grade (Fig. 3H,I).

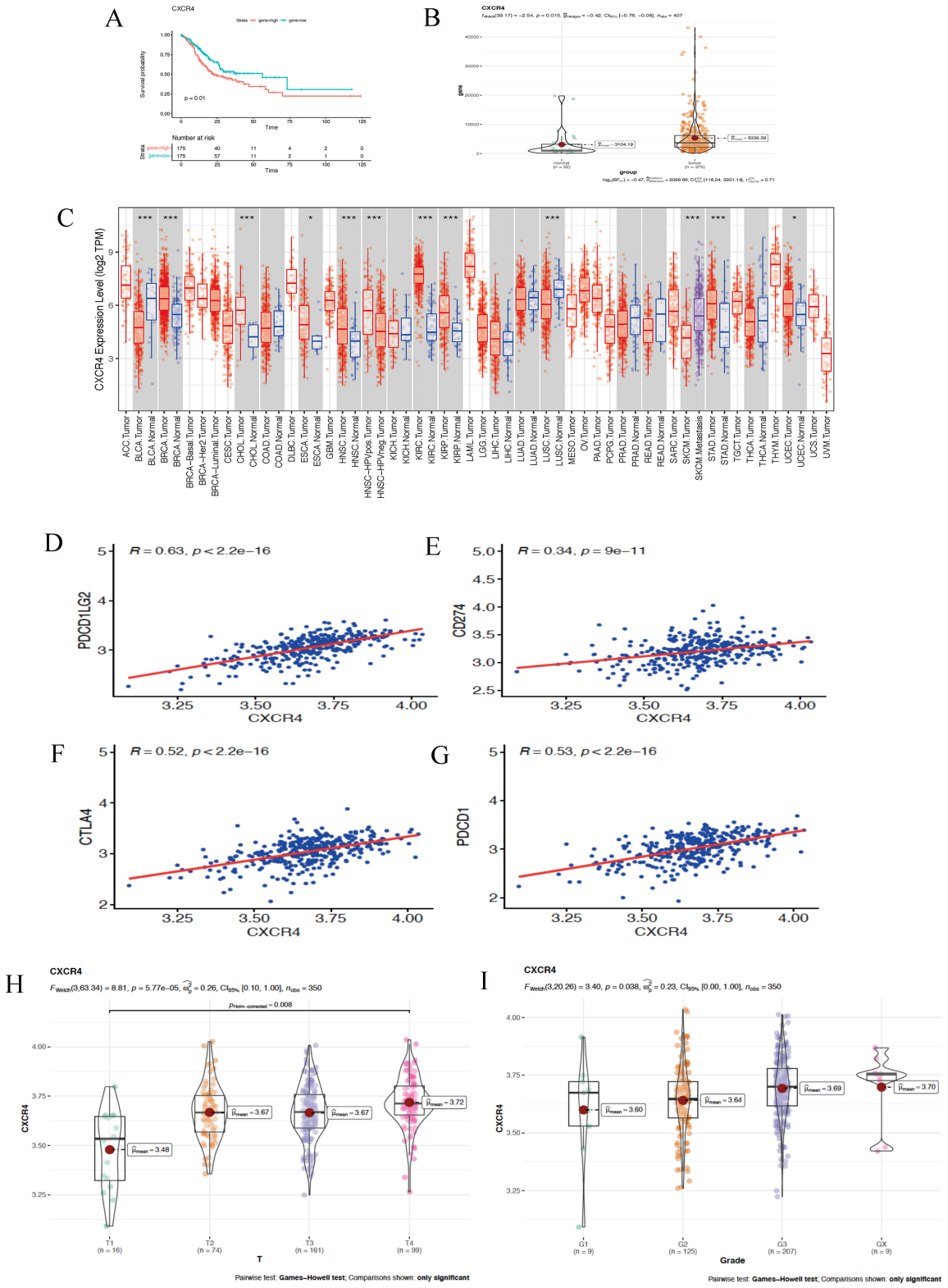

Fig. 3. Correlations between *CXCR4* expression and clinical characteristics and immune checkpoints. (A) Kaplan–Meier analysis shows that high *CXCR4* expression was significantly correlated with worse overall survival (OS) in the The Cancer Genome Atlas (TCGA) database. (B) *CXCR4* expression in the tumor samples was significantly higher than the normal samples in TCGA database. (C) The expression of *CXCR4* in pan-cancer from the TCGA database. (D–G) *CXCR4* expression was positively correlated with CTLA4, PDCD1 and PDCD1LG2 in GC samples. *CXCR4* expression was significantly correlated with T stage (H) and grade (I) in GC samples. * $p < 0.05$; *** $p < 0.001$.

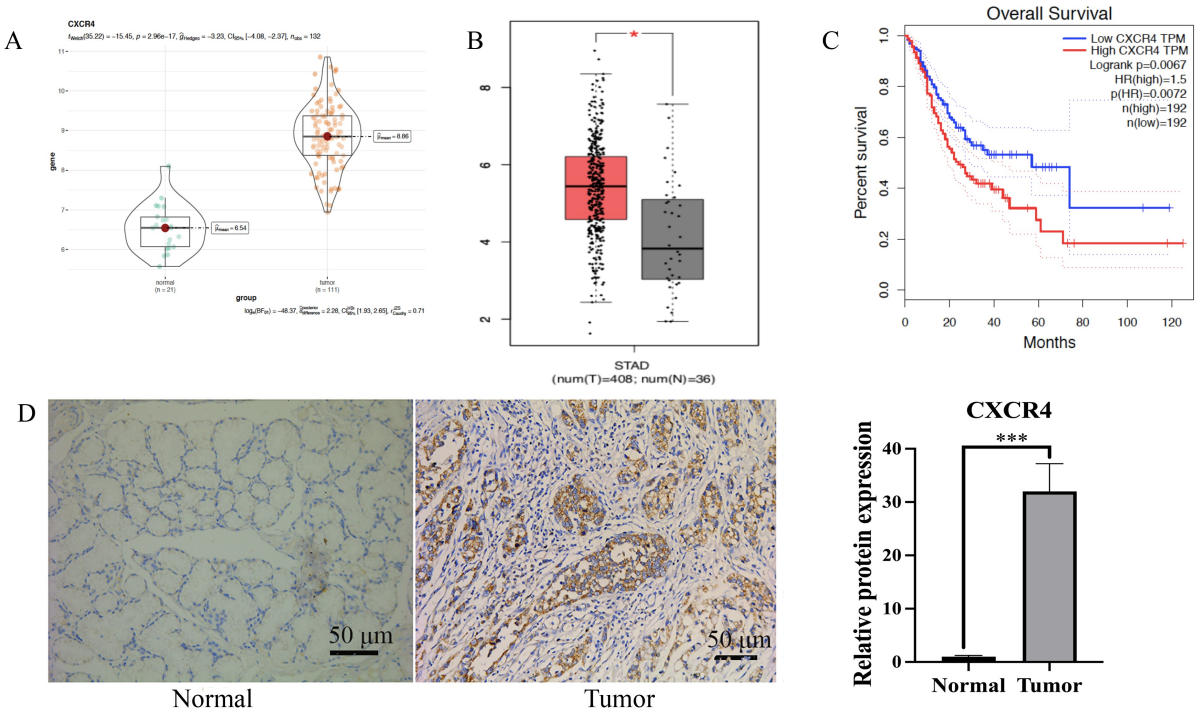

Fig. 4. Verification of expression and prognosis of *CXCR4* in GC. (A) Box plots for *CXCR4* expression in the GSE54129 dataset. (B) Box plots for *CXCR4* expression in GC from GEPIA database. (C) Survival analysis of *CXCR4* expression in GC from the GEPIA database. (D) Immunohistochemical staining for *CXCR4*. *CXCR4* was highly expressed in GC tissues compared with adjacent normal tissues. n = 3, * $p < 0.05$, *** $p < 0.001$.

Verification of Expression and Prognosis of CXCR4 in GC

To determine the expression and prognosis of *CXCR4* in GC, the GSE54129 cohort was employed to explore expression of *CXCR4*. The result shows that the *CXCR4* was highly expressed in the tumor group (Fig. 4A). A similar result was obtained concerning expression of *CXCR4* in GC from the GEPIA database ($p < 0.05$, Fig. 4B). Furthermore, the high *CXCR4* expression was also associated with unfavorable survival outcomes compared to the low-expression group from the GEPIA database (Fig. 4C). In our IHC staining, *CXCR4* was upregulated in GC tissues ($p < 0.001$, Fig. 4D).

Correlation between CXCR4 Expression and Immunotherapy

To study whether there were differences in the TME immune cell infiltration between the different *CXCR4* groups, we evaluated the phenotypic landscape of 22 types of immune cells using CIBERSORT. As the result shows, the infiltration levels of memory B cells, eosinophils, macrophages M0, activated mast cells, resting mast cells, and plasma cells were dramatically different between different *CXCR4* groups (Fig. 5A). Our data demonstrated that immune, stromal, and ESTIMATE scores in the high-*CXCR4* group were dramatically increased compared to those in the group with low *CXCR4* level ($p < 0.001$; Fig. 5B). Furthermore, the high-stromal-score group displayed markedly worse overall survival ($p < 0.05$; Fig. 5C). Similarly, the, high-ESTIMATE-score group also displayed worse overall survival ($p < 0.05$; Fig. 5D). The low-immune-score group displayed longer median overall survival compared with the high-immune-score group (18.47 months versus 14.97 months, $p = 0.17$; Fig. 5E).

ICB therapy has shown significant efficacy in the treatment of tumors in recent years. Our data indicated that TMB in the low-*CXCR4* group was significantly greater than that in high-*CXCR4* expression group (Fig. 5F), indicating that patients with low *CXCR4* level may benefit more from ICB treatment. Moreover, in the 348 GC patients, 90.8% of the individuals in the high-*CXCR4* group had genetic mutations (Fig. 5G), while 96.55% of individuals in the low-expression group had genetic mutations (Fig. 5H). This result also suggests that immunotherapy is more effective in patients with low *CXCR4* expression. Therefore, *CXCR4* can be used as an indicator to evaluate the response to ICB therapy.

Enrichment Analysis of CXCR4 Involved in Signaling Pathways in GC

To explore *CXCR4* involvement in cancer-related signaling pathways, pathway enrichment analysis was conducted using GSVA. The high-*CXCR4* group showed a marked enrichment of T helper, T cytotoxic, B lymphocyte,

monocyte, and CTLA4 pathways (Fig. 5I), indicating that *CXCR4* is important for regulation of the immune microenvironment in GC.

CXCR4 Promoted the Proliferation of GC Cells

To explore oncogenic function of *CXCR4*, we selected GC cell line HGC-27 for further experiments. HGC-27 cells were transfected with si-*CXCR4* to inhibit the expression of *CXCR4* (**Supplementary Fig. 3**). After transfection with si-*CXCR4* for 24 h, cell viability was investigated by MTT assay. Our result demonstrated that cell viability was significantly inhibited after transfection with si-*CXCR4* ($p < 0.001$, Fig. 6A). The scratch test (Fig. 6B) and transwell assay (Fig. 6C) showed that migratory ability and invasive ability were significantly suppressed after inhibiting the expression of *CXCR4* ($p < 0.001$). After transfection with si-*CXCR4* for 48 h, apoptosis was determined. Our results showed that the apoptosis of GC cells was significantly increased after inhibiting the expression of *CXCR4* ($p < 0.001$, Fig. 6D).

Discussion

The global incidence and mortality of GC are increasing year by year [18,22]. Although there are more and more treatments for GC, the survival rate of advanced GC is still low even with comprehensive treatment, mainly based on surgery [23].

Autophagy plays an important role in the oncogenesis and development of tumors. In recent years, more and more clinical trials have confirmed the role of autophagy in tumor treatment [4,9]. Therefore, targeting autophagy will be an effective tumor treatment. In our study, the expressions of autophagy-related genes were investigated. We explored the implications for prognosis, the immune microenvironment, and clinical characteristics in GC. Based on the autophagy-related gene sets, GC samples were clustered into three distinct subclasses. GC patients in subclass 2 and subclass 3 had a good overall survival, while those in subclass 1 had a poor prognosis. In addition, immune checkpoints and immune cell infiltration were significantly different among the three subtypes. Thus, our findings suggest that autophagy-related genes play a key role in the progression and prognosis of GC.

A total of 28 autophagy-related genes were differentially expressed in GC samples. However, 8 autophagy-related genes were statistically significant in univariate cox regression analysis. Among the 8 DEGs, only *CXCR4* was significantly upregulated ($p < 0.05$, $\log_2$FC >1). Moreover, *CXCR4* had the highest positive correlation with CD274 in the 8 DEGs. Besides, high *CXCR4* expression was significantly correlated with worse overall survival. Therefore, our results showed that *CXCR4* was a potential biomarker of survival, and an indicator of immunotherapy, for GC. Our results are consistent with previous research. Dali Zhao *et al*. [24] reported that *CXCR4* expression was associated with poor prognosis in hepatocellular carcinoma. Alimohammadi *et al*. [25] reported that *CXCR4* expression predicted poor prognosis in patients with malignant melanoma, indicating that *CXCR4* was a carcinogenic gene. To further clarify the role of *CXCR4* in cancer, we conducted a pan-cancer analysis. The pan-cancer analysis results revealed that *CXCR4* was significantly upregulated in many types of cancer, and high expression of *CXCR4* was correlated with poor prognosis. To explore the clinical value of *CXCR4* in different clinical variables, we found that *CXCR4* expression was significantly correlated with T stage and grade. In *in vitro* experiments, we silenced expression of *CXCR4* in GC cells by siRNA. Our results showed that silencing *CXCR4* suppressed the growth, invasion, and migration capacities of GC cells. Moreover, inhibition of *CXCR4* expression can promote the apoptosis of GC cells. Consequently, targeting *CXCR4* may be an effective therapeutic approach for GC treatment.

Immune microenvironment is important to tumor development and immunotherapy [26,27]. Autophagy can change the tumor immune response to treatment by regulating the expression of chemokines in tumor cells and the migration of immune cells to tumor [9,12]. Nagarsheth *et al*. [28] reported that Atg5-inactivated $Kras^{G12D}$-driven lung cancer cells expressed high protein levels of CXCL5 and promoted cells growth. Görgülü K *et al*. [29] reported that monoallelic Atg5-deleted $Kras^{G12D}$-driven pancreatic cancer cells can produce high levels of chemokines to attract more macrophages into pancreatic tumor tissue. In our study, we found that *CXCR4* expression was distinctly related to fractions of memory B cells, eosinophils, macrophages M0, activated mast cells, resting mast cells, and plasma cells in GC. Moreover, our results showed that immune, stromal, and ESTIMATE scores in the high-*CXCR4* expression group were significantly higher than those in the group with low *CXCR4* expression. In addition, the high-stromal-score and high-ESTIMATE-score groups displayed significantly worse overall survival. Although there was no statistically significant difference in overall survival between the high-immune-score group and the low-immune-score group, the low-immune-score group showed longer median overall survival compared with high-immune-score group (18.47 months versus 14.97 months, $p = 0.17$). *CXCR4* may be involved in remodeling of the immune microenvironment in GC, affecting the tumor prognosis and the efficacy of immunotherapy.

In recent years, ICB therapy has been considered one of the most successful methods in the treatment of cancer [30]. However, the prediction of efficacy for ICB therapy is still limited by a lack of definite biomarkers. TMB and PD-L1 IHC staining are classic ICB response indicators [31, 32]. The higher the TMB score, the better the response to immunotherapy. In our study, we found that TMB score in the low-*CXCR4*-expression group was significantly higher

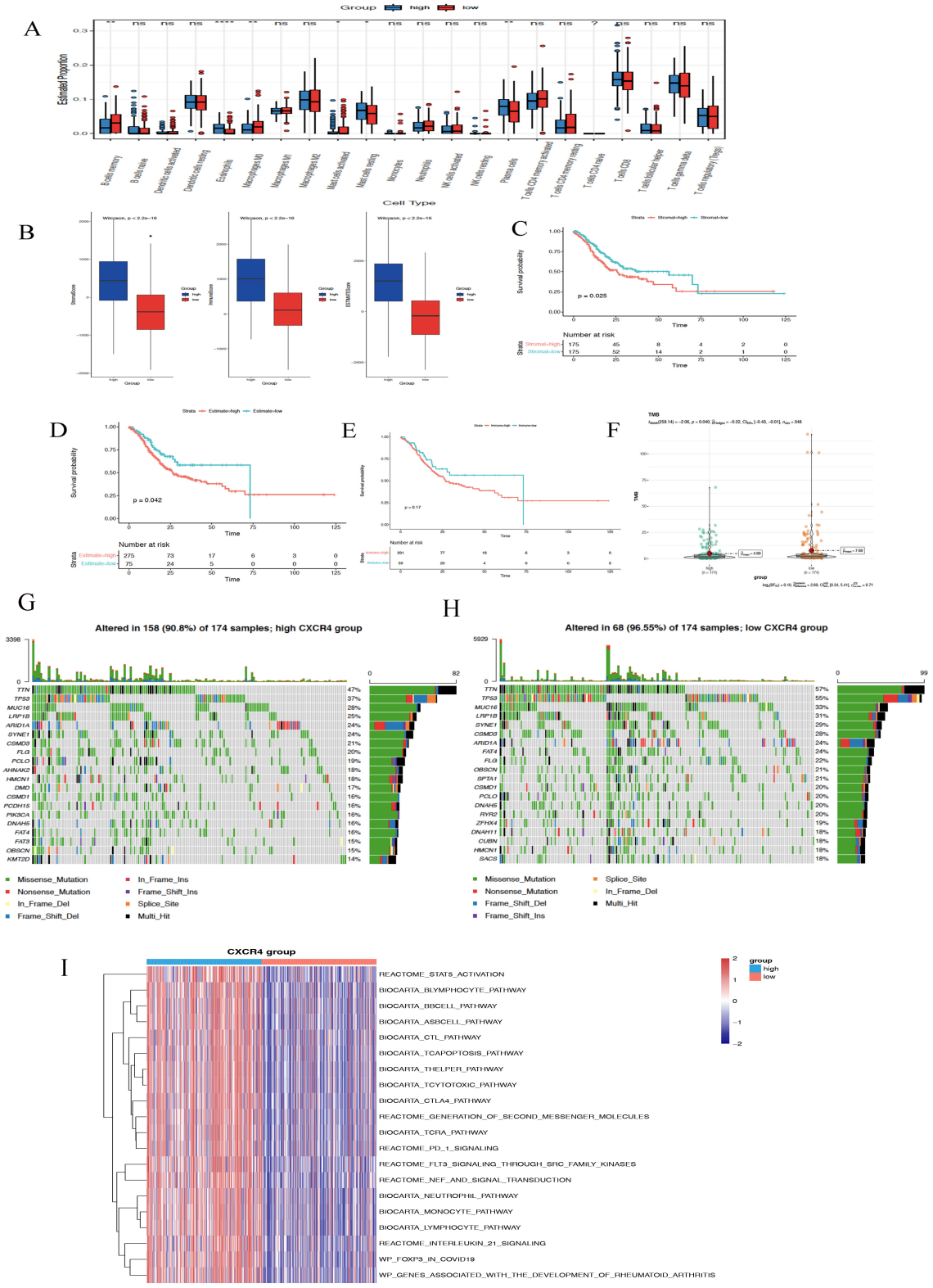

Fig. 5. Correlations between *CXCR4* expression and the immune microenvironment and somatic mutations. (A) Relationship between immune cell infiltration and *CXCR4* level. (B) The difference in stromal, immune, and estimate scores between *CXCR4* groups. Survival analyses for stromal (C), estimate (D), and immune (E) scores between different *CXCR4* groups using Kaplan–Meier curves. (F) Box plots for the association between *CXCR4* level and TMB score. The top 20 genes based on mutation frequency in high-*CXCR4* (G) and low-*CXCR4* (H) expression groups. (I) The difference in enriched pathways in different *CXCR4* groups. * $p < 0.05$; ** $p < 0.01$; **** $p < 0.0001$; ns, not significant.

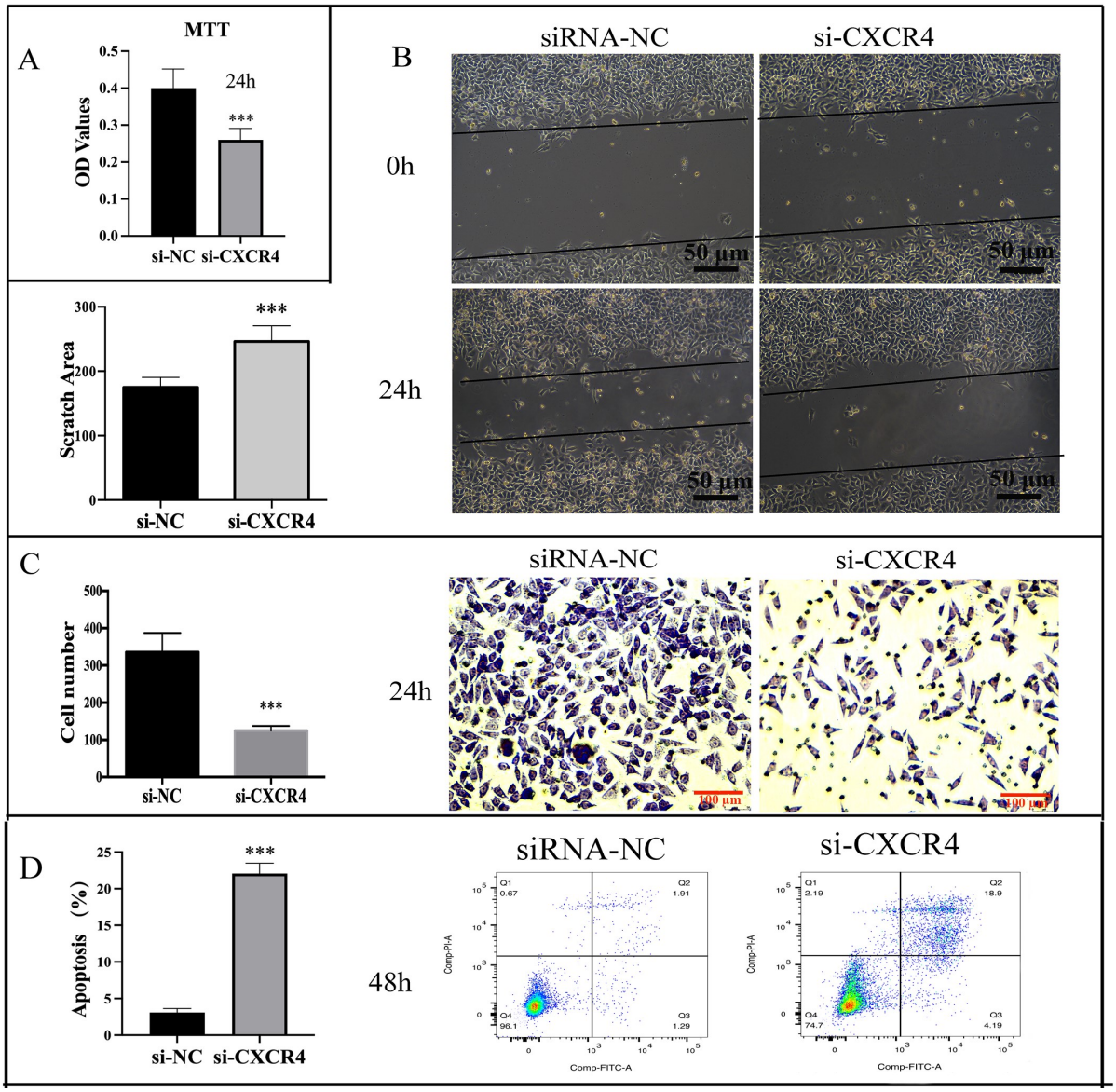

Fig. 6. *CXCR4* promotes proliferation of GC cells. (A) MTT assay. (B) The scratch test was used to assess migration of GC cells after transfection with si-*CXCR4*. (C) The migration and invasion of GC cells treated with si-*CXCR4*. (D) The apoptosis of GC cells treated with si-*CXCR4*. *** $p < 0.001$. siRNA, small interfering RNA. MTT, 3-(4,5-Dimethylthiazol-2-yl)-2,5-diphenyltetrazolium bromide.

than that in the high-*CXCR4*-expression group, indicating that patients with low *CXCR4* expression were more likely to benefit from ICB treatment.

Somatic mutations can accumulate throughout the lifetime, but the most well-known disease caused by somatic mutations is cancer [33]. Somatic mutations can cause tumor cells to produce mutant proteins that are not produced by normal cells [34]. These mutant protein sequences are degraded into short peptides that are presented to the cell surface. These are recognized as foreign antigens by T cells. Therefore, in recent years, these aberrant mutant proteins have come to be recognized as opportunities for the immune system to recognize and control tumor growth. It is evident from the clinical data that the frequency of somatic mutations is closely associated with the efficacy of ICB therapy [35]. In our study, we found that there were differences in somatic mutation frequency between high- and low-expression groups. In 348 GC patients, 90.8% of the patients in high-*CXCR4*-expression group had genetic mutations, while 96.55% of the patients in the low-expression group had genetic mutations. This result also shows that the low-*CXCR4*-expression group may benefit more from immunotherapy.

CXCR4 binds specifically to its ligand CXCL12, which can activate a series of downstream intracellular signal transduction pathways, and then regulate the biological behaviors of cell survival, proliferation, migration, and adhesion [17]. To further analyze underlying molecular mechanisms of *CXCR4* in GC, we conducted pathway enrichment analysis. Our data demonstrated that high *CXCR4*

group showed a marked enrichment of the T helper, T cytotoxic, B lymphocyte, monocyte, and CTLA4 pathways. Gil *et al*. [36] reported that *CXCR4* promoted tumor immune evasion by recruiting Treg. Chen *et al*. [37] reported that inhibition of *CXCR4* increases cytotoxic T lymphocytes (CTLs) infiltration. Obermajer *et al*. [38] reported that *CXCR4* promoted ovarian cancer progression by recruiting T regulatory and plasmacytoid dendritic immune cells. Therefore, *CXCR4* is related to regulation of the immune microenvironment. Because inhibition of autophagy represses tumor growth and improves the efficacy of other anticancer drugs, targeting *CXCR4* may be an effective therapeutic approach for GC treatment.

Conclusions

We summarized expression patterns of autophagy-related genes and explored their effects on the prognosis, immune microenvironment, and clinical features of gastric cancer. Among them, high expression of *CXCR4* was significantly related to poor prognosis. *CXCR4* is closely related to tumor progression and the tumor immune microenvironment. Therefore, *CXCR4* could be an ideal target for gastric cancer treatment.

Availability of Data and Materials

The datasets presented in the study can be found in The Cancer Genome Atlas (TCGA) data portal (https://portal.gdc.cancer.gov/) and the Gene Expression Omnibus (GEO) repository (https://www.ncbi.nlm.nih.gov/geo/). Further inquiries can be directed to the corresponding authors.

Author Contributions

ZZ and NL designed the research study. ZZ and QLF performed the research. LQW, JQL, and RPS provided help and advice on the IHC staining experiments. ZZ and NL analyzed the data. All authors contributed to editorial changes in the manuscript. All authors read and approved the final manuscript. All authors have participated sufficiently in the work and agreed to be accountable for all aspects of the work.

Ethics Approval and Consent to Participate

The study protocol was approved by the Ethics and Scientific Committee of the Guilin people's hospital (GPH202100321) and conforms to the Declaration of Helsinki. All patients and their families provided informed written consent for their information to be stored in the hospital database and used for research before surgery.

Acknowledgment

Not applicable.

Funding

This study was supported by the National Natural Science Foundation of China (grant number: 82060561), the Natural Science Foundation of Guangxi Province (grant number: 2018GXNSFBA050047), Guilin Science and Technology Projects (grant number: 20190218-7-2), and Innovation Project of Guangxi Graduate Education (grant number: YCSW2022379).

Conflict of Interest

The authors declare no conflict of interest.

Supplementary Material

Supplementary material associated with this article can be found, in the online version, at https://doi.org/10.24976/Discov.Med.202335179.115.

References

[1] Smyth EC, Nilsson M, Grabsch HI, van Grieken NC, Lordick F. Gastric cancer. Lancet. 2020; 396: 635–648.
[2] Thrift AP, El-Serag HB. Burden of Gastric Cancer. Clinical Gastroenterology and Hepatology. 2020; 18: 534–542.
[3] Patel TH, Cecchini M. Targeted Therapies in Advanced Gastric Cancer. Current Treatment Options in Oncology. 2020; 21: 70.
[4] Klionsky DJ, Petroni G, Amaravadi RK, Baehrecke EH, Ballabio A, Boya P, *et al*. Autophagy in major human diseases. The EMBO Journal. 2021; 40: e108863.
[5] Fukuda T, Wada-Hiraike O. The Two-Faced Role of Autophagy in Endometrial Cancer. Frontiers in Cell and Developmental Biology. 2022; 10: 839416.
[6] Morad G, Helmink BA, Sharma P, Wargo JA. Hallmarks of response, resistance, and toxicity to immune checkpoint blockade. Cell. 2021; 184: 5309–5337.
[7] Zhou B, Gao Y, Zhang P, Chu Q. Acquired Resistance to Immune Checkpoint Blockades: The Underlying Mechanisms and Potential Strategies. Frontiers in Immunology. 2021; 12: 693609.
[8] Khononov I, Jacob E, Fremder E, Dahan N, Harel M, Raviv Z, *et al*. Host response to immune checkpoint inhibitors contributes to tumor aggressiveness. Journal for Immunotherapy of Cancer. 2021; 9: e001996.
[9] Xia H, Green DR, Zou W. Autophagy in tumour immunity and therapy. Nature Reviews. Cancer. 2021; 21: 281–297.
[10] Jiang H, Courau T, Borison J, Ritchie AJ, Mayer AT, Krummel MF, *et al*. Activating Immune Recognition in Pancreatic Ductal Adenocarcinoma via Autophagy Inhibition, MEK Blockade, and CD40 Agonism. Gastroenterology. 2022; 162: 590–603.e14.
[11] Limagne E, Nuttin L, Thibaudin M, Jacquin E, Aucagne R, Bon M, *et al*. MEK inhibition overcomes chemoimmunotherapy resistance by inducing CXCL10 in cancer cells. Cancer Cell. 2022; 40: 136–152.e12.
[12] Yamamoto K, Venida A, Yano J, Biancur DE, Kakiuchi M, Gupta S, *et al*. Autophagy promotes immune evasion of pancreatic cancer by degrading MHC-I. Nature. 2020; 581: 100–105.
[13] Cheung PF, Yang J, Fang R, Borgers A, Krengel K, Stoffel A, *et al*. Progranulin mediates immune evasion of pancreatic ductal adenocarcinoma through regulation of MHCI expression. Nature Communications. 2022; 13: 156.

[14] Mukhopadhyay S, Mahapatra KK, Praharaj PP, Patil S, Bhutia SK. Recent progress of autophagy signaling in tumor microenvironment and its targeting for possible cancer therapeutics. Seminars in Cancer Biology. 2022; 85: 196–208.

[15] Yang N, Chen T, Wang L, Liu R, Niu Y, Sun L, *et al*. *CXCR4* mediates matrix stiffness-induced downregulation of UBTD1 driving hepatocellular carcinoma progression via YAP signaling pathway. Theranostics. 2020; 10: 5790–5801.

[16] Ottaiano A, Santorsola M, Del Prete P, Perri F, Scala S, Caraglia M, *et al*. Prognostic Significance of *CXCR4* in Colorectal Cancer: An Updated Meta-Analysis and Critical Appraisal. Cancers. 2021; 13: 3284.

[17] Jiang X, Zheng J, Liu L, Jiang K, Wen Y, Yan Y, *et al*. *CXCR4* is a Novel Biomarker Correlated With Malignant Transformation and Immune Infiltrates in Gastric Precancerous Lesions. Frontiers in Molecular Biosciences. 2021; 8: 697993.

[18] Li K, Zhang A, Li X, Zhang H, Zhao L. Advances in clinical immunotherapy for gastric cancer. Biochimica et Biophysica Acta. Reviews on Cancer. 2021; 1876: 188615.

[19] Danilova L, Ho WJ, Zhu Q, Vithayathil T, De Jesus-Acosta A, Azad NS, *et al*. Programmed Cell Death Ligand-1 (PD-L1) and CD8 Expression Profiling Identify an Immunologic Subtype of Pancreatic Ductal Adenocarcinomas with Favorable Survival. Cancer Immunology Research. 2019; 7: 886–895.

[20] Zhao Z, Han F, Yang S, Wu J, Zhan W. Oxamate-mediated inhibition of lactate dehydrogenase induces protective autophagy in gastric cancer cells: involvement of the Akt-mTOR signaling pathway. Cancer Letters. 2015; 358: 17–26.

[21] Zhao Z, Han F, He Y, Yang S, Hua L, Wu J, *et al*. Stromal-epithelial metabolic coupling in gastric cancer: stromal MCT4 and mitochondrial TOMM20 as poor prognostic factors. European Journal of Surgical Oncology. 2014; 40: 1361–1368.

[22] Yeoh KG, Tan P. Mapping the genomic diaspora of gastric cancer. Nature Reviews. Cancer. 2022; 22: 71–84.

[23] Huang S, Ma L, Lan B, Liu N, Nong W, Huang Z. Comprehensive analysis of prognostic genes in gastric cancer. Aging. 2021; 13: 23637–23651.

[24] Zhao D, Yang Z, Chen C, Zhang Z, Yu Y, Li Z. *CXCR4* promotes gefitinib resistance of Huh7 cells by activating the c-Met signaling pathway. FEBS Open Bio. 2021; 11: 3115–3125.

[25] Alimohammadi M, Rahimi A, Faramarzi F, Alizadeh-Navaei R, Rafiei A. Overexpression of chemokine receptor *CXCR4* predicts lymph node metastatic risk in patients with melanoma: A systematic review and meta-analysis. Cytokine. 2021; 148: 155691.

[26] Mao X, Xu J, Wang W, Liang C, Hua J, Liu J, *et al*. Crosstalk between cancer-associated fibroblasts and immune cells in the tumor microenvironment: new findings and future perspectives. Molecular Cancer. 2021; 20: 131.

[27] Liu K, Cui JJ, Zhan Y, Ouyang QY, Lu QS, Yang DH, *et al*. Reprogramming the tumor microenvironment by genome editing for precision cancer therapy. Molecular Cancer. 2022; 21: 98.

[28] Nagarsheth N, Wicha MS, Zou W. Chemokines in the cancer microenvironment and their relevance in cancer immunotherapy. Nature Reviews. Immunology. 2017; 17: 559–572.

[29] Görgülü K, Diakopoulos KN, Ai J, Schoeps B, Kabacaoglu D, Karpathaki AF, *et al*. Levels of the Autophagy-Related 5 Protein Affect Progression and Metastasis of Pancreatic Tumors in Mice. Gastroenterology. 2019; 156: 203–217.e20.

[30] Helmink BA, Reddy SM, Gao J, Zhang S, Basar R, Thakur R, *et al*. B cells and tertiary lymphoid structures promote immunotherapy response. Nature. 2020; 577: 549–555.

[31] Samstein RM, Lee CH, Shoushtari AN, Hellmann MD, Shen R, Janjigian YY, *et al*. Tumor mutational load predicts survival after immunotherapy across multiple cancer types. Nature Genetics. 2019; 51: 202–206.

[32] Jardim DL, Goodman A, de Melo Gagliato D, Kurzrock R. The Challenges of Tumor Mutational Burden as an Immunotherapy Biomarker. Cancer Cell. 2021; 39: 154–173.

[33] Mustjoki S, Young NS. Somatic Mutations in "Benign" Disease. The New England Journal of Medicine. 2021; 384: 2039–2052.

[34] Yarchoan M, Johnson BA, 3rd, Lutz ER, Laheru DA, Jaffee EM. Targeting neoantigens to augment antitumour immunity. Nature Reviews. Cancer. 2017; 17: 569.

[35] Zhang N, Zhang J, Wang G, He X, Mi Y, Cao Y, *et al*. Predictive Efficacy of Blood-Based Tumor Mutation Burden Assay for Immune Checkpoint Inhibitors Therapy in Non-Small Cell Lung Cancer: A Systematic Review and Meta-Analysis. Frontiers in Oncology. 2022; 12: 795933.

[36] Gil M, Komorowski MP, Seshadri M, Rokita H, McGray AJR, Opyrchal M, *et al*. CXCL12/*CXCR4* blockade by oncolytic virotherapy inhibits ovarian cancer growth by decreasing immunosuppression and targeting cancer-initiating cells. Journal of Immunology (Baltimore, Md.: 1950). 2014; 193: 5327–5337.

[37] Chen IX, Chauhan VP, Posada J, Ng MR, Wu MW, Adstamongkonkul P, *et al*. Blocking *CXCR4* alleviates desmoplasia, increases T-lymphocyte infiltration, and improves immunotherapy in metastatic breast cancer. Proceedings of the National Academy of Sciences of the United States of America. 2019; 116: 4558–4566.

[38] Obermajer N, Muthuswamy R, Odunsi K, Edwards RP, Kalinski P. PGE(2)-induced CXCL12 production and *CXCR4* expression controls the accumulation of human MDSCs in ovarian cancer environment. Cancer Research. 2011; 71: 7463–7470.